Entanglement Hamiltonian of Interacting Fermionic Models

Francesco Parisen Toldin* and Fakher F. Assaad†
Institut für Theoretische Physik und Astrophysik, Universität Würzburg, Am Hubland, D-97074 Würzburg, Germany

(Received 26 April 2018; revised manuscript received 12 July 2018; published 14 November 2018)

Recent numerical advances in the field of strongly correlated electron systems allow the calculation of the entanglement spectrum and entropies for interacting fermionic systems. An explicit determination of the entanglement (modular) Hamiltonian has proven to be a considerably more difficult problem, and only a few results are available. We introduce a technique to directly determine the entanglement Hamiltonian of interacting fermionic models by means of auxiliary field quantum Monte Carlo simulations. We implement our method on the one-dimensional Hubbard chain partitioned into two segments and on the Hubbard two-leg ladder partitioned into two chains. In both cases, we study the evolution of the entanglement Hamiltonian as a function of the physical temperature.

DOI: 10.1103/PhysRevLett.121.200602

Introduction.—The advent of quantum information techniques in the field of condensed matter physics has boosted a variety of new insights in old and new problems. In particular, recent years have witnessed a rapidly growing number of investigations of the quantum entanglement in strongly correlated many-body systems [1,2]. The simplest approach is the so-called bipartite entanglement, where one divides a system into two parts, and a reduced density matrix describing one of the subsystems is obtained by tracing out the degrees of freedom of the other part. Arguably, the most studied quantities in this context are the entropies of the reduced density matrix, that is, the von Neumann and especially the Renyi entropies. In the ground state, the entanglement entropies generically satisfy an area law; i.e., to leading order they are proportional to the area between the two subsystems [3]. Among the many results, it is well established that in a $1+1$ conformal field theory (CFT) corrections to the area law allow one to extract the central charge of a model [4].

More information is contained in the entanglement Hamiltonian, also known as the modular Hamiltonian, which is defined as the negative logarithm of the reduced density matrix. Its spectrum, dubbed as the "entanglement spectrum," has been shown to feature the edge physics of topologically ordered phases such as the fractional quantum Hall state [5] as well as of symmetry-protected topological states of matter [2,6–9]. The entanglement Hamiltonian also plays a central role in the first law of entanglement [10]. Beside the entanglement spectrum and the associated eigenvectors, the knowledge of the entanglement Hamiltonian opens the possibility of characterizing the reduced density matrix as a thermal state. Furthermore, the expectation value of the entanglement Hamiltonian equals the von Neumann entanglement entropy, a key quantity which is generically not accessible in numerical simulations of interacting models. Perhaps not surprisingly, compared to the computation of entanglement entropies, an explicit determination of the entanglement Hamiltonian has proven to be a considerably more difficult problem, and only a few solvable results are available. Aside from limiting cases, such as in the absence of interactions between the two subsystems, or the high-temperature limit, where the entanglement Hamiltonian can be easily determined, a particularly important result concerns a relativistic field theory in flat d-dimensional Minkowski space. For a bipartition of the space into two semi-infinite subsystems with no corners, translationally invariant along $d-1$ dimensions, the entanglement Hamiltonian is given by an integral of the energy-momentum tensor, with a weight proportional to the distance x from the boundary, leading to the Bisognano-Wichmann (BW) form of the entanglement Hamiltonian [11,12]. In the presence of additional conformal symmetry, a mapping of the semi-infinite space to a ball allows one again to express the entanglement Hamiltonian as an integral of the energy-momentum tensor, with a space-dependent weight [13]. Reference [14] provides a recent review of the cases in $1+1$ CFT where the entanglement Hamiltonian is obtained as a weighted integral of the energy-momentum tensor.

Concerning condensed matter models on a lattice, the entanglement Hamiltonian is exactly known only in a few cases in one dimension and for a semi-infinite line subsystem: the noncritical transverse-field Ising model and the XXZ model in the massive phase [15,16]. Even in the deceptively simple case of a free (nonrelativistic) fermionic chain, the explicit computation of the entanglement Hamiltonian for a segment proved to be a rather difficult task. Although for a free fermionic system an exact formula for the entanglement Hamiltonian is known [17], its explicit calculation for a finite segment embedded in a chain has eluded an analytical treatment so far. All lattice models mentioned above share the property of being described by a

CFT in the low-energy limit; hence the entanglement Hamiltonian should attain the BW form, as indeed confirmed by the exact determination for the Ising and XXZ models. Nevertheless, the entanglement Hamiltonian of the free fermionic chain model contains intriguing corrections to the CFT prediction which, remarkably, persist even in the limit of a long segment [18]. In this context, recent studies have provided numerical evidence in support of a lattice-discretized BW form of the entanglement Hamiltonian for various models in both one and two dimensions [19–23].

In this Letter, we introduce a numerically exact quantum Monte Carlo (QMC) method which allows one to determine the entanglement Hamiltonian of interacting model of fermions. The method is applied to the Hubbard chain and to the two-leg Hubbard ladder, where we compute the one- and two-body terms of the entanglement Hamiltonian as a function of the temperature.

Method.—The method presented here is based on QMC simulations using the auxiliary field algorithm [24–26], whose basic formulation is reported in the following. The Hamiltonian of the system $\hat{H}$ is separated into a sum of a free part $\hat{T}$ (containing, e.g., hopping terms) and an interaction part $\hat{V}$ (e.g., a Hubbard repulsion). At finite inverse temperature β, one introduces a Trotter decomposition of the density matrix operator $\exp(-\beta\hat{H})$; in the models considered here, we found important to choose a symmetric decomposition $\exp(-\beta\hat{H}) = [\exp(-\Delta\tau\hat{T}/2) \times \exp(-\Delta\tau\hat{V})\exp(-\Delta\tau\hat{T}/2)]^N + O(\Delta\tau^2)$, with $\beta = N\Delta\tau$ thereby ensuring the Hermiticity of the imaginary time propagation. Then, the interaction term is decoupled via a Hubbard-Stratonovich (HS) decomposition, introducing discrete HS fields $\{s\}$. The QMC simulation consists in a stochastic sampling of the probability distribution $P(\{s\})$ associated with the HS fields. The ALF package provides a framework to program auxiliary field QMC simulations [27]. The introduction of the HS transformation results in a free fermionic system in the HS fields $\{s\}$. For such a system, the reduced density matrix associated with a subpartition A of the Hilbert space can be written exactly in terms of the Green's functions of the model, restricted to the subsystem A [28]. One then arrives to the following expression for the reduced density matrix $\hat{\rho}_A$ [29]:

$$\hat{\rho}_A = \int d\{s\} P(\{s\}) \det[\mathbb{1} - G_A(\{s\})] e^{-\hat{\boldsymbol{a}}_i^\dagger h_{ij}(\{s\})\hat{\boldsymbol{a}}_j},$$
$$h(\{s\}) = \log\{[G_A(\{s\})^T]^{-1} - \mathbb{1}\}, \tag{1}$$

where $\hat{\boldsymbol{a}}_i^\dagger$ and $\hat{\boldsymbol{a}}_i$ are the fermionic creation and annihilation operators, respectively, in the subsystem A and i and j are superindices labeling the possible states in A; here and in the following, we assume an implicit summation over repeated indices. The Green's function matrix $G_A(\{s\})_{ij} \equiv \langle \hat{\boldsymbol{a}}_i^\dagger \hat{\boldsymbol{a}}_j \rangle$ restricted to A, and at a given configuration of $\{s\}$, is readily accessible in the auxiliary field algorithm, and it is computed at a fixed imaginary-time slice. Equation (1) has been exploited to compute the Renyi entropies [8,29–31]. Alternatively, Renyi entropies can be computed by means of the replica trick, in fermionic [9,32–34] and bosonic [35] as well as spin systems [36,37].

Equation (1) suggests to introduce a new measure $\widetilde{P}(\{s\}) \propto P(\{s\}) \det[\mathbb{1} - G_A(\{s\})]$, such that $\hat{\rho}_A$ is obtained as an expectation value over the measure $\widetilde{P}(\{s\})$:

$$\hat{\rho}_A \propto \langle e^{-\hat{\boldsymbol{a}}_i^\dagger h_{ij}(\{s\})\hat{\boldsymbol{a}}_j} \rangle_{\widetilde{P}}. \tag{2}$$

As discussed in Supplemental Material [38], for the models considered here it can be proven that $P(\{s\})$ as well as the determinant $\det[\mathbb{1} - G_A(\{s\})]$ are positive; hence, $\widetilde{P}(\{s\})$ can be sampled by QMC simulations without a sign problem. Furthermore, as proven in Ref. [38], the exponential on the right-hand side of Eq. (2) admits an expansion in normal-ordered many-body operators:

$$e^{-\hat{\boldsymbol{a}}_i^\dagger h_{ij}(\{s\})\hat{\boldsymbol{a}}_j} = 1 + \hat{\boldsymbol{a}}_i^\dagger (e^{-h(\{s\})} - \mathbb{1})_{ij} \hat{\boldsymbol{a}}_j + \frac{1}{2}\hat{\boldsymbol{a}}_i^\dagger \hat{\boldsymbol{a}}_k^\dagger (e^{-h(\{s\})} - \mathbb{1})_{ij} (e^{-h(\{s\})} - \mathbb{1})_{kl} \hat{\boldsymbol{a}}_l \hat{\boldsymbol{a}}_j + \cdots. \tag{3}$$

By inserting Eq. (3) in Eq. (2), we obtain an expansion of $\hat{\rho}_A$ as a sum of many-body operators, whose coefficients can be sampled with a QMC simulation. This gives us an unbiased QMC determination of $\hat{\rho}_A$.

In order to compute the entanglement Hamiltonian $\hat{H}_E$, we first calculate the matrix elements M of $\hat{\rho}_A$. The matrix $N \equiv -\log(M)$ represents, by definition, the matrix elements of $\hat{H}_E$. The entanglement Hamiltonian is then obtained by determining the many-body operator whose matrix elements are N. As for $\hat{\rho}_A$, we expand $\hat{H}_E$ as a sum of normal-ordered many-body operators:

$$\hat{H}_E = -\log(\hat{\rho}_A) = \text{const} - \hat{\boldsymbol{a}}_i^\dagger t_{ij} \hat{\boldsymbol{a}}_j + \hat{\boldsymbol{a}}_i^\dagger \hat{\boldsymbol{a}}_k^\dagger U_{ijkl} \hat{\boldsymbol{a}}_l \hat{\boldsymbol{a}}_j + \cdots. \tag{4}$$

Crucially, it is possible to prove that, in order to compute $\hat{H}_E$ up to the two-body term $\hat{\boldsymbol{a}}_i^\dagger \hat{\boldsymbol{a}}_k^\dagger U_{ijkl} \hat{\boldsymbol{a}}_l \hat{\boldsymbol{a}}_j$, it is sufficient to truncate the sampling of $\hat{\rho}_A$ to the two-body term, as done on the right-hand side of Eq. (3). Under this condition, the computational cost for sampling $\hat{\rho}_A$ and determining $\hat{H}_E$ is only polynomial in the size of the subsystem A. As discussed in Ref. [38], the expansion of Eqs. (3) and (4) can be extended to any order in a sum of normal-ordered many-body operators, whose coefficients could be, in principle, sampled as to determine $\hat{\rho}_A$ and $\hat{H}_E$ beyond the two-body terms. More technical details on this step of the algorithm, implemented using the TRIQS [39] and ARMADILLO [40,41] libraries, are reported in Ref. [38].

Results.—We have applied the method outlined above to the Hubbard chain and the Hubbard two-leg ladder at half filling. The Hamiltonian for a Hubbard chain of length L is

$$\hat{H} = -t \sum_{i=1,\sigma}^{L} \hat{c}^{\dagger}_{i,\sigma}\hat{c}_{i+1,\sigma} + \hat{c}^{\dagger}_{i+1,\sigma}\hat{c}_{i,\sigma} + U \sum_{i=1}^{L} \left(\hat{n}_{i,\uparrow} - \frac{1}{2}\right)\left(\hat{n}_{i,\downarrow} - \frac{1}{2}\right), \qquad \sigma = \uparrow, \downarrow, \tag{5}$$

where by imposing periodic boundary conditions we identify the lattice site $L+1$ with 1. For this model, we cut a subsystem A consisting in a segment of length L_a and compute the one-body term t_{ij} defined in Eq. (4). In Fig. 1, we show the resulting hopping terms $t_{i,i+1}$ between nearest-neighbor lattice sites i and $i+1$, as a function of i and for three inverse temperatures $\beta = 1$, 2, and 3. At a high temperature $\beta = 1$, we find that $t_{i,i+1}$ attains the value of 1 for all lattice sites except those next to the boundary. In fact, if the entanglement between A and B is locally restricted to a region close to the boundaries, we expect that, away from such a region, the subsystem A is substantially independent of B, and, hence, locally, the entanglement Hamiltonian should match $\beta\hat{H}_A$, with $\hat{H}_A$ the Hamiltonian of the model, restricted to A. Accordingly, we observe a plateau with $t_{i,i+1} \simeq \beta t = \beta$ in the central part of the plots in Fig. 1, whose extension shrinks as the temperature is lowered and the entanglement grows. For $\beta = 3$ only for a single site in the middle we find $t_{i,i+1} \simeq \beta$, whereas close to the boundaries we observe an approximately linear dependence of $t_{i,i+1}$ on i, which grows (respectively, decreases) when close to the left (respectively, right) boundary. Such a behavior resembles qualitatively the case of a CFT [14]. For the Hamiltonian parameters considered, the other hopping terms in $\hat{H}_E$ are negligible. For reasons expanded upon in Ref. [38], it is technically hard, for this specific model, to reach lower temperatures and especially to investigate temperature scales below which the magnetic correlation length is substantial. Nevertheless, as a comparison in order to reproduce the results of Fig. 1 by exact diagonalization (ED) techniques, one would need a full-spectrum diagonalization of a Hubbard chain with size $L = 32$, a task far beyond current ED capabilities.

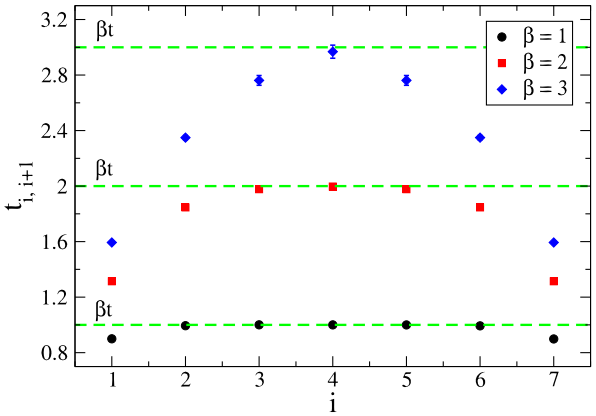

FIG. 1. Nearest-neighbor hopping terms of the entanglement Hamiltonian for a segment of $L_a = 8$ sites in a Hubbard chain of total length $L = 32$, and parameters $t = 1$ and $U = 4$, as a function of the temperature. The dashed line indicates the expected values far from the boundary; see the main text.

In contrast, for the Hubbard model on a two-leg ladder, we were able to reach *low* temperatures, approaching the ground state. The Hamiltonian is defined as

$$\hat{H} = -t \sum_{\substack{i,\sigma \\ O=A,B}} \hat{c}^{\dagger}_{i,O,\sigma}\hat{c}_{i+1,O,\sigma} + \hat{c}^{\dagger}_{i+1,O,\sigma}\hat{c}_{i,\sigma} - t_{\perp} \sum_{i,\sigma} \hat{c}^{\dagger}_{i,A,\sigma}\hat{c}_{i,B,\sigma} + \hat{c}^{\dagger}_{i,B,\sigma}\hat{c}_{i,A,\sigma} + U \sum_{i,O=A,B} \left(\hat{n}_{i,O,\uparrow} - \frac{1}{2}\right)\left(\hat{n}_{i,O,\downarrow} - \frac{1}{2}\right), \tag{6}$$

where t and $t_{\perp}$ indicate the intra- and interleg hopping constants, respectively, and A and B label the two legs. For this geometry, we trace out one leg and obtain a translationally invariant entanglement Hamiltonian for a single leg, i.e., defined on a chain geometry. At half filling, the ground state of the model consists of a single fully gapped phase [42,43]. The charge gap Δ_C and the spin gap Δ_S, with $\Delta_C > \Delta_S$, are monotonically increasing with $t_{\perp}$ and U. Gapped systems exhibit, as a function of the linear size, a fast approach to the thermodynamic limit [44,45].

Figure 2 illustrates the temperature dependence of the nearest-neighbor hopping term $t_{i,i+1}$ in $\hat{H}_E$ for $t_{\perp} = 2$ and 2.5 and fixed coupling constants $t = 1$ and $U = 4$. At high temperatures, $t_{i,i+1}$ grows linearly with β, $t_{i,i+1} \simeq \beta t$, in

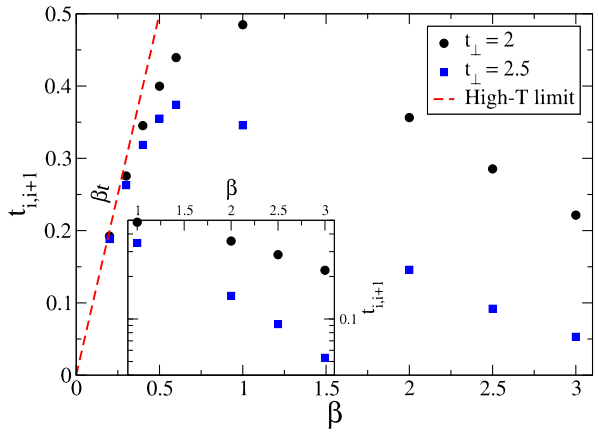

FIG. 2. The same as Fig. 1, for a Hubbard two-leg ladder of linear length $L = 8$, with fixed parameters $t = 1$ and $U = 4$, as a function of the temperature for two values of $t_{\perp}$. The dashed line indicates the expected high-temperature limit $t_{i,i+1} \simeq \beta t$. The inset shows a magnification of the plot for $\beta \geq 1$ in a semilogarithmic scale.

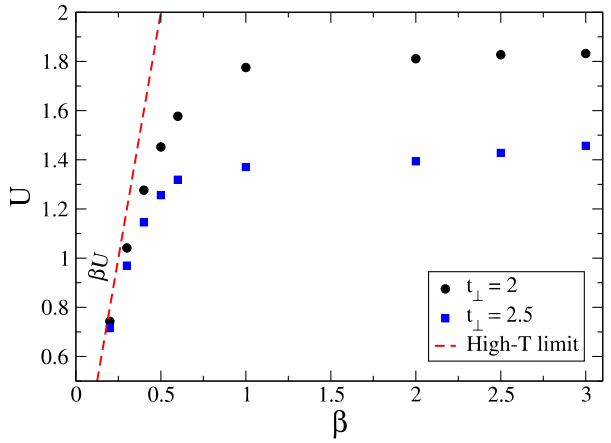

FIG. 3. The same as Fig. 2 for the on-site Hubbard repulsion U.

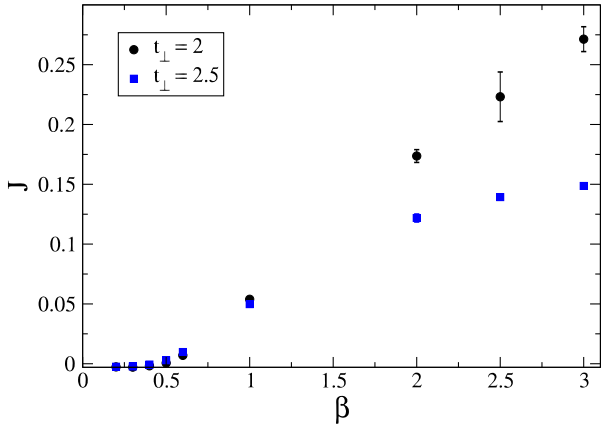

FIG. 4. The same as Fig. 2 for the nearest-neighbor spin-spin interaction J.

agreement with the theoretical expectation $\hat{H}_E = \text{const} + \beta\hat{H}_A + O(\beta^2)$, $\beta \to 0$, which follows easily by Taylor expanding the density matrix $\rho \sim \exp(-\beta\hat{H})$ to the lowest order in β. Upon decreasing the temperature, one eventually crosses the charge and spin gaps, leading to a suppression of the charge fluctuations. The entanglement Hamiltonian reflects this physics, showing a nonmonotonic temperature dependence of $t_{i,i+1}$, which starts to decrease for large enough values of β. The value of β at which $t_{i,i+1}$ stops to grow decreases upon increasing $t_\perp$, because the gaps increase with $t_\perp$ [42,43]. Figure 2 confirms this observation. Furthermore, a semilog plot of the data shown in the inset in Fig. 2 supports an exponential suppression of the hopping constants $t_{i,i+1}$ for $\beta \to \infty$. We notice that the charge gaps and spin gaps are $\Delta_C \approx 1.6$ and $\Delta_S \approx 0.6$ for $t_\perp = 2$ and $\Delta_C \approx 2.1$ and $\Delta_S \approx 1.3$ for $t_\perp = 2.5$ [42], respectively; hence, the data in Fig. 2 for the largest values of β are well below the gaps and essentially approach the ground state of the model. Hopping terms $t_{i,i+x}$ at distances $x > 1$ are negligible compared to the nearest-neighbor one $t_{i,i+1}$.

For this model, we are able to compute all two-body terms in $\hat{H}_E$. In Fig. 3, we show the on-site Hubbard repulsion term U. As for the hopping term, it exhibits the expected linear increase with β for high temperatures. However, upon crossing the gaps, U saturates to a $t_\perp$-dependent value. The entanglement Hamiltonian contains also interaction terms which are absent in Eq. (6), such as a nearest-neighbor antiferromagnetic spin-spin interaction $J\vec{S}_i\vec{S}_{i+1}$ and a next-nearest-neighbor ferromagnetic interaction $J'\vec{S}_i\vec{S}_{i+2}$, displayed in Figs. 4 and 5. Both J and J' vanish at high temperatures, as expected, and grow only when the temperature is below the gaps of the model. Additional two-body terms such as particle-particle interactions $V_{ij}\hat{\boldsymbol{n}}_i\hat{\boldsymbol{n}}_i$ and spin-spin interactions at distances larger than 2 are effectively negligible compared to those shown in Figs. 3–5. All in all, the entanglement Hamiltonian exhibits a remarkable crossover between a Hubbard-like Hamiltonian at high temperatures, where $\hat{H}_E \simeq \beta\hat{H}_A + \text{const}$ to a Heisenberg-like Hamiltonian at low temperatures, where $U \gg t$ and additional nonfrustrating spin-spin interactions J and J' enforce an antiferromagnetic order. Such a behavior is analog to what is found in the two-leg Heisenberg model, where, for antiferromagnetic interchain and intra-chain couplings, the entanglement spectrum matches the one for a Heisenberg chain [46,47], as confirmed also by perturbative calculations showing that for strong rung coupling the entanglement Hamiltonian is approximately proportional to the restriction of the Hamiltonian to a single leg [48–50]; similar results have been obtained, e.g., in the case of free fermions [48], bilayer quantum Hall systems [51], and Hofstadter bilayers [52] (see also Ref. [53] and references therein). We notice that our results outperform ED, because a full spectrum diagonalization of a Hubbard model, needed to reproduce Figs. 2–5, is currently feasible for lattices with $N \lesssim 12$ sites [54], corresponding to a $L = 6$ two-leg ladder.

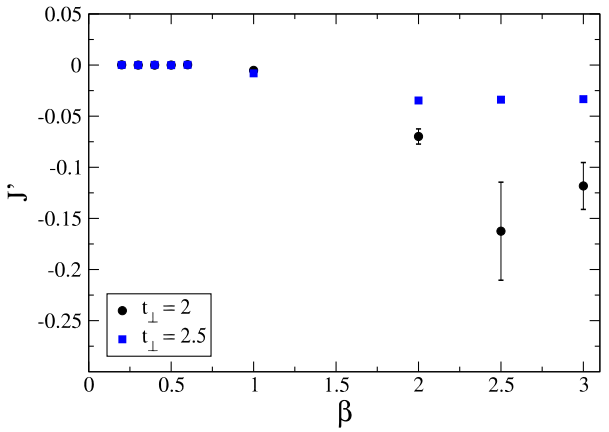

FIG. 5. The same as Fig. 2 for the next-nearest-neighbor spin-spin interaction J'.

Summary.—In this Letter, we present a general framework for computing the reduced density matrix and the entanglement Hamiltonian of an interacting fermionic model. The method is formulated within the auxiliary field QMC method, and allows one to unbiasedly determine the reduced density matrix and the entanglement Hamiltonian as a series of normal-ordered many-body operators. The method is applied to the Hubbard chain and two-leg models, where we present the first numerically exact determination of the one-body and two-body terms of the entanglement Hamiltonian. The results clearly show the increase of correlations and entanglement upon lowering the temperature, and for the two-leg model a change in the physical behavior of the model upon crossing the gaps, with the emergence of qualitatively different interactions in the entanglement Hamiltonian. Our results outperform current ED techniques; in fact, even if the ground state or the full spectrum is obtained by ED, the determination of the entanglement Hamiltonian requires the highly numerically unstable computation of the logarithm of the reduced density matrix. Thus, we expect our findings to provide a benchmark for future studies. The generality of the method described here paves the way for future investigations of interacting models, where the knowledge of the entanglement Hamiltonian may provide new useful insights. In fact, almost all of the entanglement measures can be, in principle, obtained from the entanglement Hamiltonian. Its determination with the present method can then allow one to compute key quantities otherwise inaccessible to numerical simulations, such as the entanglement negativity and the von Neumann entanglement entropy, which is simply equal to the expectation value of the entanglement Hamiltonian. The method lends itself to study the reduced density matrix for a subsystem A embedded into a potentially large system B. Thus, one may investigate the extension and space dependence of entanglement by, e.g., considering a possibly small, spatially disconnected, subsystem A.

F. P. T. is grateful to Igor Krivenko for technical support on the TRIQS library [39] and to Didier Poilblanc and German Sierra Rodero for useful discussions. We thank Andreas Läuchli and John Schliemann for useful communications. F. P. T. thanks the German Research Foundation (DFG) through Grant No. AS120/13-1 of the FOR 1807. F. F. A. thanks the DFG for financial support through the SFB 1170 ToCoTronics. We acknowledge the computing time granted by the John von Neumann Institute for Computing (NIC) and provided on the supercomputer JURECA [55] at the Jülich Supercomputing Center.

*francesco.parisentoldin@physik.uni-wuerzburg.de
†assaad@physik.uni-wuerzburg.de

[1] N. Laflorencie, Quantum entanglement in condensed matter systems, Phys. Rep. **646**, 1 (2016).
[2] F. Parisen Toldin and F. F. Assaad, Entanglement studies of interacting fermionic models, arXiv:1810.06595.
[3] J. Eisert, M. Cramer, and M. B. Plenio, Colloquium: Area laws for the entanglement entropy, Rev. Mod. Phys. **82**, 277 (2010).
[4] P. Calabrese and J. Cardy, Entanglement entropy and quantum field theory, J. Stat. Mech. (2004) P06002.
[5] H. Li and F. D. M. Haldane, Entanglement Spectrum as a Generalization of Entanglement Entropy: Identification of Topological Order in Non-Abelian Fractional Quantum Hall Effect States, Phys. Rev. Lett. **101**, 010504 (2008).
[6] L. Fidkowski, Entanglement Spectrum of Topological Insulators and Superconductors, Phys. Rev. Lett. **104**, 130502 (2010).
[7] A. M. Turner, Y. Zhang, and A. Vishwanath, Entanglement and inversion symmetry in topological insulators, Phys. Rev. B **82**, 241102 (2010).
[8] F. F. Assaad, T. C. Lang, and F. P. Toldin, Entanglement spectra of interacting fermions in quantum Monte Carlo simulations, Phys. Rev. B **89**, 125121 (2014).
[9] F. F. Assaad, Stable quantum Monte Carlo simulations for entanglement spectra of interacting fermions, Phys. Rev. B **91**, 125146 (2015).
[10] D. D. Blanco, H. Casini, L.-Y. Hung, and R. C. Myers, Relative entropy and holography, J. High Energy Phys. 08 (2013) 060.
[11] J. J. Bisognano and E. H. Wichmann, On the duality condition for a Hermitian scalar field, J. Math. Phys. (N.Y.) **16**, 985 (1975).
[12] J. J. Bisognano and E. H. Wichmann, On the duality condition for quantum fields, J. Math. Phys. (N.Y.) **17**, 303 (1976).
[13] H. Casini, M. Huerta, and R. C. Myers, Towards a derivation of holographic entanglement entropy, J. High Energy Phys. 05 (2011) 036.
[14] J. Cardy and E. Tonni, Entanglement Hamiltonians in two-dimensional conformal field theory, J. Stat. Mech. (2016) 123103.
[15] H. Itoyama and H. B. Thacker, Lattice Virasoro Algebra and Corner Transfer Matrices in the Baxter Eight-Vertex Model, Phys. Rev. Lett. **58**, 1395 (1987).
[16] I. Peschel, M. Kaulke, and Ö. Legeza, Density-matrix spectra for integrable models, Ann. Phys. (Leipzig) **8**, 153 (1999).
[17] I. Peschel, On the reduced density matrix for a chain of free electrons, J. Stat. Mech. (2004) P06004.
[18] V. Eisler and I. Peschel, Analytical results for the entanglement Hamiltonian of a free-fermion chain, J. Phys. A **50**, 284003 (2017).
[19] P. Kim, H. Katsura, N. Trivedi, and J. H. Han, Entanglement and corner Hamiltonian spectra of integrable open spin chains, Phys. Rev. B **94**, 195110 (2016).
[20] M. Dalmonte, B. Vermersch, and P. Zoller, Quantum simulation and spectroscopy of entanglement Hamiltonians, Nat. Phys. **14**, 827 (2018).
[21] A. Kosior, M. Lewenstein, and A. Celi, Unruh effect for interacting particles with ultracold atoms, arXiv:1804.11323.
[22] W. Zhu, Z. Huang, and Y.-c. He, Reconstructing entanglement Hamiltonian via entanglement eigenstates, arXiv:1806.08060.

[23] G. Giudici, T. Mendes-Santos, P. Calabrese, and M. Dalmonte, Entanglement Hamiltonians of lattice models via the Bisognano-Wichmann theorem, Phys. Rev. B **98**, 134403 (2018).
[24] R. Blankenbecler, D. J. Scalapino, and R. L. Sugar, Monte Carlo calculations of coupled boson-fermion systems. I, Phys. Rev. D **24**, 2278 (1981).
[25] S. R. White, D. J. Scalapino, R. L. Sugar, E. Y. Loh, J. E. Gubernatis, and R. T. Scalettar, Numerical study of the two-dimensional Hubbard model, Phys. Rev. B **40**, 506 (1989).
[26] F. F. Assaad and H. Evertz, World-Line and Determinantal Quantum Monte Carlo Methods for Spins, Phonons and Electrons, in *Computational Many-Particle Physics*, Lecture Notes in Physics, edited by H. Fehske, R. Schneider, and A. Weiße (Springer, Berlin, 2008), Vol. 739, pp. 277–356, doi: 10.1007/978-3-540-74686-7_10.
[27] M. Bercx, F. Goth, J. S. Hofmann, and F. F. Assaad, The ALF (Algorithms for Lattice Fermions) project release 1.0. Documentation for the auxiliary field quantum Monte Carlo code, SciPost Phys. **3**, 013 (2017).
[28] I. Peschel, Calculation of reduced density matrices from correlation functions, J. Phys. A **36**, L205 (2003).
[29] T. Grover, Entanglement of Interacting Fermions in Quantum Monte Carlo Calculations, Phys. Rev. Lett. **111**, 130402 (2013).
[30] J. E. Drut and W. J. Porter, Hybrid Monte Carlo approach to the entanglement entropy of interacting fermions, Phys. Rev. B **92**, 125126 (2015).
[31] J. E. Drut and W. J. Porter, Entanglement, noise, and the cumulant expansion, Phys. Rev. E **93**, 043301 (2016).
[32] P. Broecker and S. Trebst, Rényi entropies of interacting fermions from determinantal quantum Monte Carlo simulations, J. Stat. Mech. (2014) P08015.
[33] L. Wang and M. Troyer, Renyi Entanglement Entropy of Interacting Fermions Calculated Using the Continuous-Time Quantum Monte Carlo Method, Phys. Rev. Lett. **113**, 110401 (2014).
[34] P. Broecker and S. Trebst, Numerical stabilization of entanglement computation in auxiliary-field quantum Monte Carlo simulations of interacting many-fermion systems, Phys. Rev. E **94**, 063306 (2016).
[35] S. V. Isakov, M. B. Hastings, and R. G. Melko, Topological entanglement entropy of a Bose-Hubbard spin liquid, Nat. Phys. **7**, 772 (2011).
[36] M. B. Hastings, I. González, A. B. Kallin, and R. G. Melko, Measuring Renyi Entanglement Entropy in Quantum Monte Carlo Simulations, Phys. Rev. Lett. **104**, 157201 (2010).
[37] S. Humeniuk and T. Roscilde, Quantum Monte Carlo calculation of entanglement Rényi entropies for generic quantum systems, Phys. Rev. B **86**, 235116 (2012).
[38] See Supplemental Material at http://link.aps.org/supplemental/10.1103/PhysRevLett.121.200602 for a discussion of the QMC sampling, a proof and generalization of Eq. (3), and a description of the procedure to explicitly evaluate Eq. (4).
[39] O. Parcollet, M. Ferrero, T. Ayral, H. Hafermann, I. Krivenko, L. Messio, and P. Seth, TRIQS: A toolbox for research on interacting quantum systems, Comput. Phys. Commun. **196**, 398 (2015).
[40] C. Sanderson and R. Curtin, Armadillo: A template-based C++ library for linear algebra, J. Open Source Software **1**, 26 (2016).
[41] C. Sanderson and R. Curtin, A User-Friendly Hybrid Sparse Matrix Class in C++, Lect. Notes Comput. Sci. **10931**, 422 (2018).
[42] R. M. Noack, S. R. White, and D. J. Scalapino, The ground state of the two-leg Hubbard ladder. A density-matrix renormalization group study, Physica (Amsterdam) **270C**, 281 (1996).
[43] Z. Weihong, J. Oitmaa, C. J. Hamer, and R. J. Bursill, Numerical studies of the two-leg Hubbard ladder, J. Phys. Condens. Matter **13**, 433 (2001).
[44] H. Neuberger, Finite size effects in massive field theory, Phys. Lett. B **233**, 183 (1989).
[45] Z. Wang, F. F. Assaad, and F. Parisen Toldin, Finite-size effects in canonical and grand-canonical quantum Monte Carlo simulations for fermions, Phys. Rev. E **96**, 042131 (2017).
[46] D. Poilblanc, Entanglement Spectra of Quantum Heisenberg Ladders, Phys. Rev. Lett. **105**, 077202 (2010).
[47] J. I. Cirac, D. Poilblanc, N. Schuch, and F. Verstraete, Entanglement spectrum and boundary theories with projected entangled-pair states, Phys. Rev. B **83**, 245134 (2011).
[48] I. Peschel and M.-C. Chung, On the relation between entanglement and subsystem Hamiltonians, Europhys. Lett. **96**, 50006 (2011).
[49] A. M. Läuchli and J. Schliemann, Entanglement spectra of coupled $S = 1/2$ spin chains in a ladder geometry, Phys. Rev. B **85**, 054403 (2012).
[50] J. Schliemann and A. M. Läuchli, Entanglement spectra of Heisenberg ladders of higher spin, J. Stat. Mech. (2012) P11021.
[51] J. Schliemann, Entanglement spectrum and entanglement thermodynamics of quantum Hall bilayers at $\nu = 1$, Phys. Rev. B **83**, 115322 (2011).
[52] J. Schliemann, Entanglement spectra and entanglement thermodynamics of Hofstadter bilayers, New J. Phys. **15**, 053017 (2013); **15**, 079501 (2013).
[53] J. Schliemann, Entanglement thermodynamics, J. Stat. Mech. (2014) P09011.
[54] A. M. Läuchli (private communication).
[55] Jülich Supercomputing Centre, JURECA: General-purpose supercomputer at Jülich Supercomputing Centre, J. Large-Scale Res. Facil. **2**, A62 (2016).